JOURNAL OF MATERIALS SCIENCE 21 (1986) 4395–4402

The initial stages of ordering in CuAuI and CuAuII

G. VAN TENDELOO, S. AMELINCKX
RUCA, University of Antwerp, Groenenborgerlaan 171, B2020 Antwerp, Belgium
S. J. JENG, C. M. WAYMAN
Department of Metallurgy and Mining Engineering, and Materials Research Laboratory, University of Illinois, Urbana, Illinois, USA

The initial ordering stages of CuAu have been studied by electron microscopy. At 250° C, in the CuAuI stability range, ordering proceeds fast and initially very little twinning is observed. At 390° C, in the CuAuII stability range, a long incubation time is required before CuAuII platelets are nucleated. (1 1 0) twinning takes place immediately after the plate formation and is observed down to the tip of the plate. The fine structure of the periodic antiphase boundaries in CuAuII is studied by HREM; it reveals the disorder along the boundary.

1. Introduction

CuAu is disordered above 410° C, it forms a long-period ordered superstructure (CuAuII) between 410 and 380° C and acquires the $L1_0$ structure (CuAuI) below 380° C. Both ordered structures are very closely related; CuAuII is orthorhombic and is derived from the tetragonal CuAuI phase by introducing periodic antiphase boundaries every Mth unit cell along the (1 0 0) planes (see Fig. 1).

For stoichiometric CuAu, M equals exactly 5 [1] or a value close to 5 but clearly distinct from 5.0 [2]. Guymont *et al.* [3] suggested that the observed value depends upon the previous heat treatment. The structure as proposed in Fig. 1 and first determined by Johansson and Linde [4] is only a first approximation of reality. Okamura *et al.* [5] found that a lattice relaxation occurs close to the boundary (copper atoms shift towards the antiphase boundary (APB); gold atoms shift away from it) and that considerable disordering takes place in the neighbourhood of the APB. Recently, Takeda and Hashimoto [6] confirmed this disordering and also found a different type of APB in thin film CuAuII. We have used high resolution electron microscopy to image the disorder along the boundaries and we intend to demonstrate that a distinction between 5.0 and 5.13 is rather insignificant.

Another problem to the solution of which we would like to contribute is the nucleation of CuAuI and CuAuII from the disordered or short-range ordered (SRO) phase. Nucleation of CuAuI has been followed using electron microscopy by Hirabayashi and Weissmann [7] and mainly the twinning due to strain accommodation has been studied. Nucleation of CuAuII proceeds very unusually, and rather contradictory explanations have been put forward by Aaronson and Kinsman [8] and Bowles and Wayman [9]. When observed by optical microscopy the transformation looks martensite-like [10] although it is, of course, an order–disorder reaction.

2. Experimental details

99.999% pure copper and 99.99% pure gold were melted together in quartz capsules under a 10^{-6} torr vacuum at 1100° C. Rods of 2.3 or 3 mm diameter were obtained by remelting in quartz capsules having the required diameter. The material was homogenized at 800° C for 5 days and specimens for electron microscopy were sliced and thinned mechanically down to 100 μm thickness after which another heat treatment for 1 h at 800° C was given. Specimens were then quenched into ice water and subsequently annealed at 390° C (in the CuAuII region) or at 250° C (in the CuAuI range) for different periods of time. In some cases direct quenching from 800 to 390° C was also applied. Electropolishing was performed by a double jet technique using 133 ml acetic acid, 7 ml water and 25 g Cr_2O_3, diluted 10 : 1 before using. The voltage was around 50 V but the current was kept constant at 200 mA. Proper rinsing afterwards in a mixture of acetic acid and water followed by water and ethyl alcohol is essential to obtain clean specimens. A 200 kV top entry electron microscope (C_S = 1.1 mm) was used for the high resolution observations and a 125 kV microscope, equipped with a double tilt specimen holder, for the other observations.

3. Initial stages of ordering in CuAuI

Studing the as-quenched state to gain information about the short-range ordered (SRO) state is an allowed and convenient solution when one can be sure that long-range ordering (LRO) is suppressed during the quench. This is the case, for example, in Au_4Cr where annealing times of several hours are required to produce small ordered domains [11, 12]. However, when CuAu is quenched from 800° C in the usual way, ordering cannot be completely avoided. The diffraction pattern exhibits diffuse intensity maxima at 1 0 0, 0 1 0 and 1 1 0 positions but no pronounced splitting of these maxima in two or four satellites as, for example,

0022–2461/86 $03.00 + .12

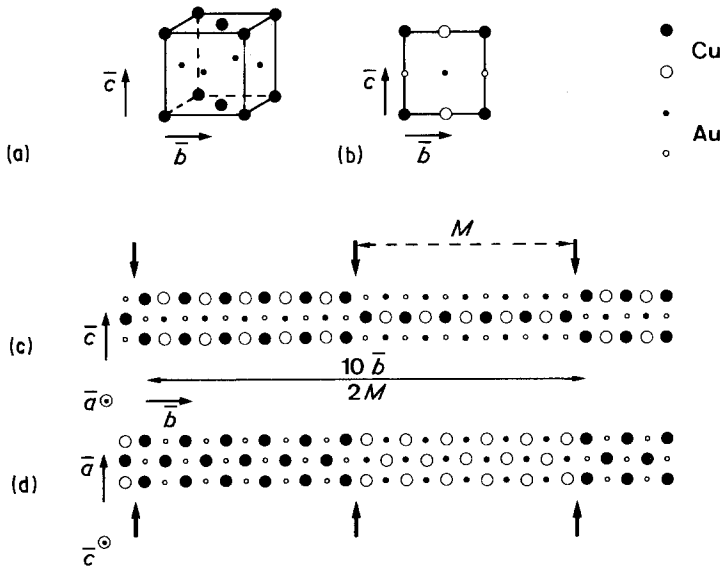

Figure 1 Structural representation of CuAuI and CuAuII: (a) spacial view of the tetragonal CuAuI; (b) CuAuI projected along the $\bar{a}$-axis; (c) CuAuII projected along the $\bar{a}$-axis; (d) CuAuII projected along the $\bar{c}$-axis.

in Cu_3Au or Cu_3Pd is observed (Fig. 2 inset). The overall symmetry of the diffraction pattern remains cubic and the basic reflections have only a slight tendency to develop a $\langle 1\,1\,0 \rangle$ type streaking. Dark-field images in the superstructure reflections reveal the presence of small ordered domains (Fig. 2a).

High-resolution bright-field images also reveal the ordering which is very localized and only extends over areas of about 2 nm wide. Bright dots form a square ordered arrangement and are separated by 0.37 nm along the [1 0 0] and [0 1 0] direction (Fig. 2b).

Ordering in CuAu proceeds very fast; when the

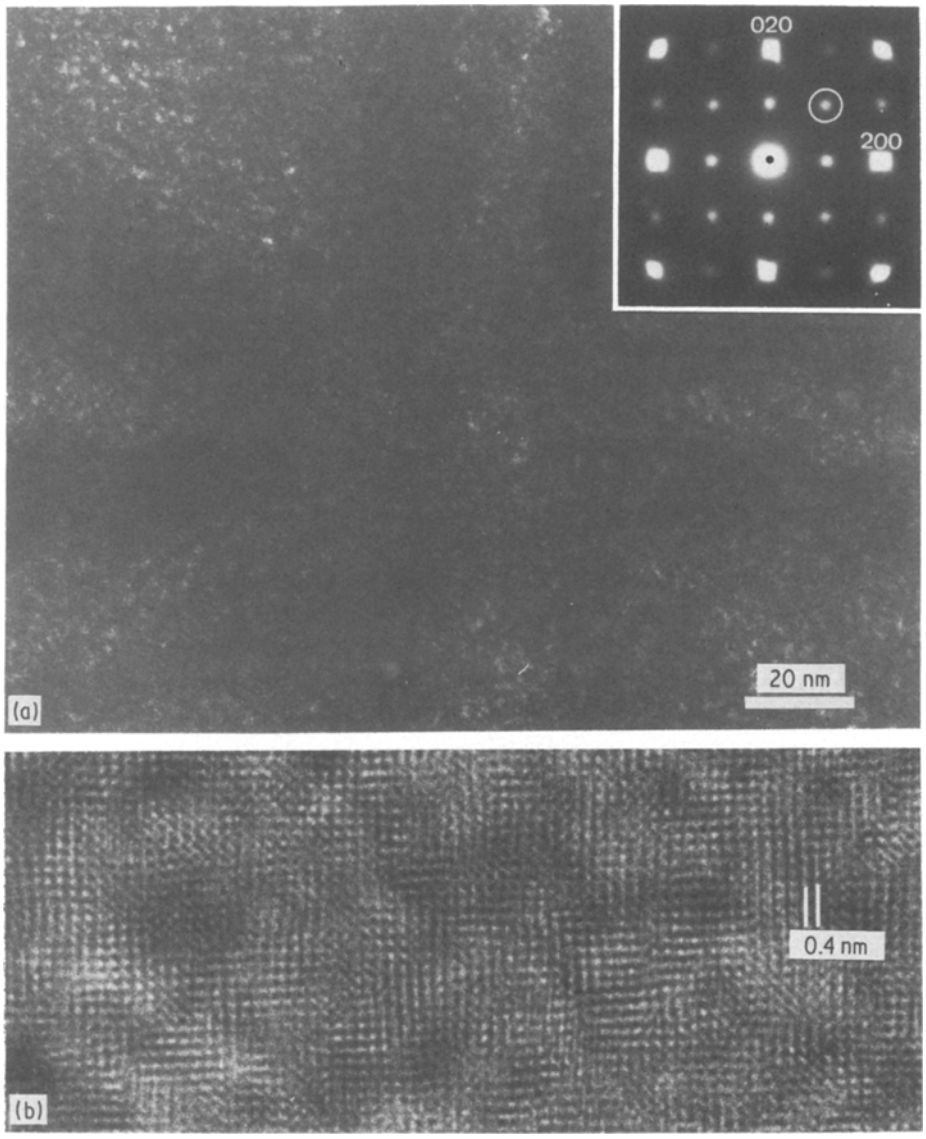

Figure 2 CuAu quenched from 800° C: (a) dark-field image in a 1 1 0 reflection (encircled in the diffraction pattern which is shown as an inset); (b) high-resolution bright-field image including all reflections up to 2 0 0 into the objective aperture.

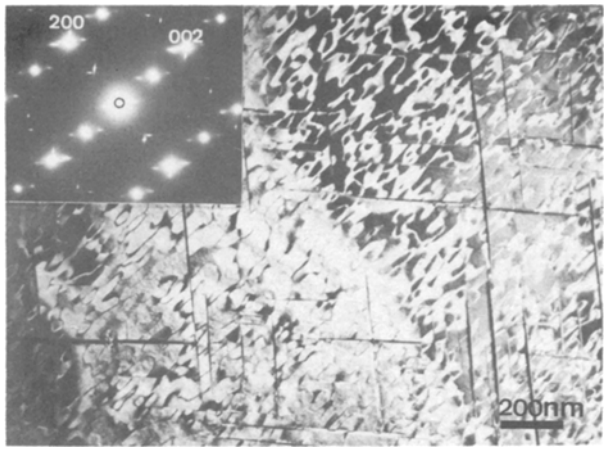

Figure 3 0 0 1 dark-field image of CuAu annealed for 5 min at 250° C. White curvy defects are APBs; black needles are small areas of different orientation variants. The corresponding diffraction pattern is shown as an inset.

quenching is performed by taking the quartz tube out of the furnace the ordered microdomains already form a pronounced texture lining up along {1 1 0} planes. Three orientation variants with their *c*-axis along the three cube directions are present. After annealing times of only 5 min at 250° C the material is completely ordered, but a large anisotropy with respect to the occurrence of the different orientation variants is noted (Fig. 3). One observes large monodomains with only occasionally very fine (1 0 1) bound platelets of the other variants. Antiphase boundaries occur very frequently and it is clear that the (1 0 1) twins generated *after* the ordering was completed since they intersect the preexisting APBs. This is certainly no thin foil effect since the heat treatment is given in the bulk material prior to electrothinning. After longer annealing times, e.g. 10 to 30 min at 250° C the number and size of such platelets has increased and the distribution of the different variants has become more isotropic (Fig. 4). The further behaviour of these twins after longer annealing times has been described in detail by Hirabayashi and Weissmann [7]. The presence of large monodomains containing a large number of

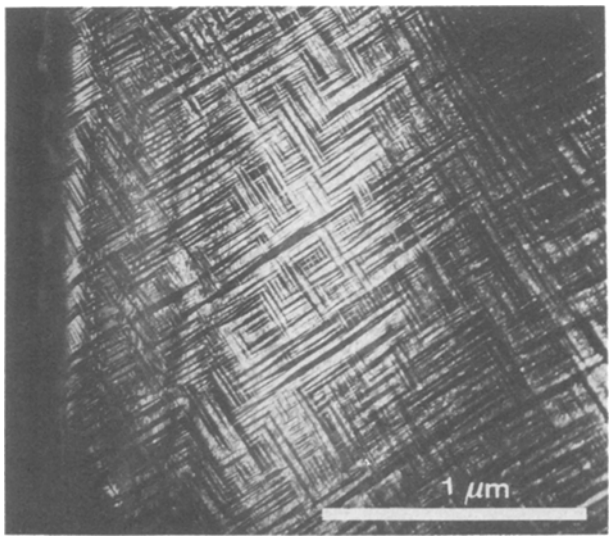

Figure 4 0 0 1 dark-field image of CuAuI annealed for 10 min at 250° C.

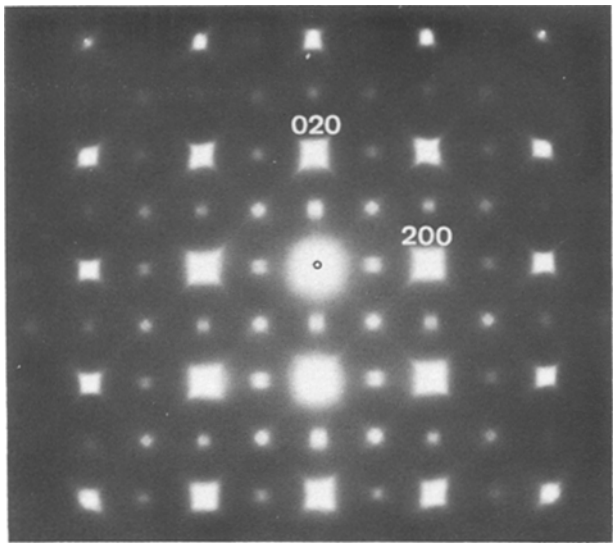

Figure 5 [0 0 1] electron diffraction pattern of CuAu annealed for 30 min at 390° C. Note the four-fold splitting of the 1 1 0 type reflections and the intense ⟨1 1 0⟩ streaking of the basic reflections.

APBs could suggest that in the initial ordering stages the c/a ratio is 1 (or very close to 1) and that only later at a more perfect order this value would decrease to 0.93 giving rise to more twinning. This, however, is not confirmed by the experiments; the measured c/a ratio from the electron diffraction pattern in Fig. 3 is $c/a = 0.91$, even less than the ideal value.

4. Initial stages of ordering of CuAuII

390° C is in the CuAuII stability range, and from the behaviour at 250° C one would expect that the ordering would proceed very fast. However, annealing for up to 30 min at this temperature does not produce any long-range order. The diffraction patterns (e.g. Fig. 5) are, nevertheless, different from the ones obtained after quenching (see Fig. 2a). The diffuse maxima at 1 1 0 are more clearly split into four satellites and somewhat less diffuse than in the quenched state. Basic reflections now acquire an intense ⟨1 1 0⟩ type streaking characteristic of "tweed" [13]. Also in the direct image the typical tweed behaviour, as described recently by Robertson and Wayman for Ni–Al [14–16] and Cu–Ni–Al [17], is observed (Fig. 6).

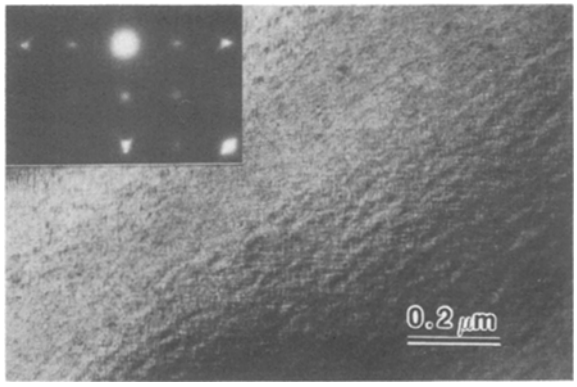

Figure 6 Bright-field image under 2 0 0 two-beam conditions in CuAu after 30 min at 390° C. The diffraction pattern into a more symmetrical [0 0 1] orientation is inserted.

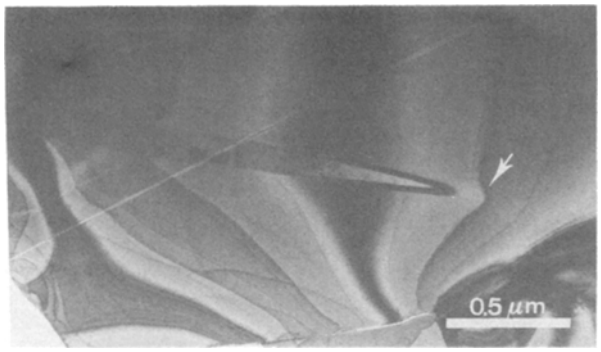

Figure 7 Nucleation of a CuAuII plate after annealing for 45 min at 390° C. Note the bending of the contours in the vicinity of the tip (see arrow).

After 30 to 45 min at 390° C CuAuII ordered platelets appear. The microstructure, as for example, in Fig. 7, has very much the appearance of a martensitic-type transformation; this has already been noticed using optical microscopy by Smith and Bowles [10]. Tweed contrast remains strong in the untransformed areas but decreases below visibility in the CuAuII platelets. At the tip of the platelets strain is concentrated; this can be deduced from the shape changes of the extinction contours around the tip (Fig. 7). Inside the plate the CuAuII structure is twinned. No twin-free zone which one might expect in the very thin CuAuII plates is observed. In Fig. 8 the twin platelets which are approximately 60 nm wide are observed up to the tip of the plate. Along the CuAuII–matrix interface dislocations are observed associated with each twin interface.

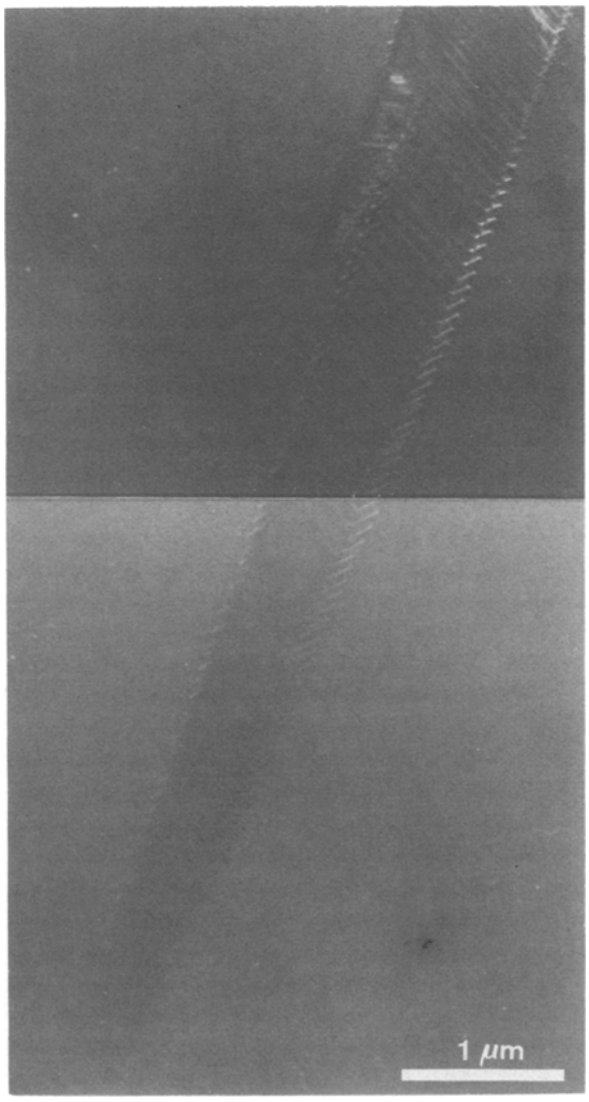

Figure 8 3 1 1 dark-field weak beam image of a CuAuII plate in a short-range ordered matrix. Note the presence of interface dislocations at the edges of the plate.

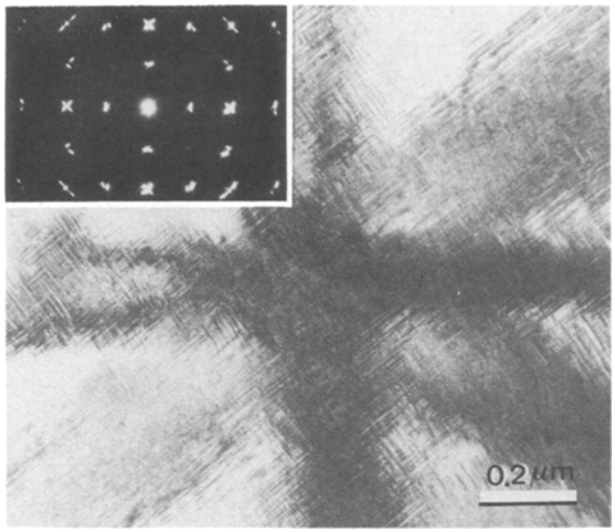

Figure 9 Ordered CuAuI plates are formed when heating quenched CuAu to 250° C. The diffraction pattern along [0 0 1] only reveals two out of three possible orientation variants. In [0 0 1]-oriented thin foils no variant having a *c*-axis parallel to the foil normal is formed.

5. *In situ* heating experiment

Several specimens quenched from 800° C have been heat treated inside the electron microscope; most specimens had an orientation close to $[0\,0\,1]_{\text{cubic}}$. The aim was to follow *in situ* the nucleation and growth of CuAuI, in the same way as was done by Penisson *et al.* [18] for Pt–Co. Because of the presence of the tweed the initial ordering stages are difficult to detect. Fine plate-shaped precipitates lying in {1 1 0} type planes start to form around 250° C and manifest themselves in the diffraction pattern by sharpening up of the 1 0 0 and 0 1 0 type reflections. In the bright-field image one observes an enhanced tweed pattern but dark-field images in 1 0 0 type reflections clearly reveal the ordered platelets. Only two out of three orientation variants form in specimens with a foil orientation close to $[0\,0\,1]_{\text{cubic}}$; the formation of the variant with its *c*-axis parallel to the foil normal is suppressed in thin foils (Fig. 9).

Upon continued heating the ordered domains grow until coalescence; the twin boundaries lie strictly in (1 0 1) planes and APBs are formed within the domains. No CuAuII is formed in the thin foils even after long annealing in the CuAuII stability range. Above T_c ordering suddenly disappears and is replaced by short-range order. The diffraction pattern shows the typical SRO reflections (Fig. 10a) and the basic reflections acquire an intense ⟨1 1 0⟩ streaking. The image also reveals a pronounced tweed texture. Dark-field images in the SRO reflections above T_c did not reveal any

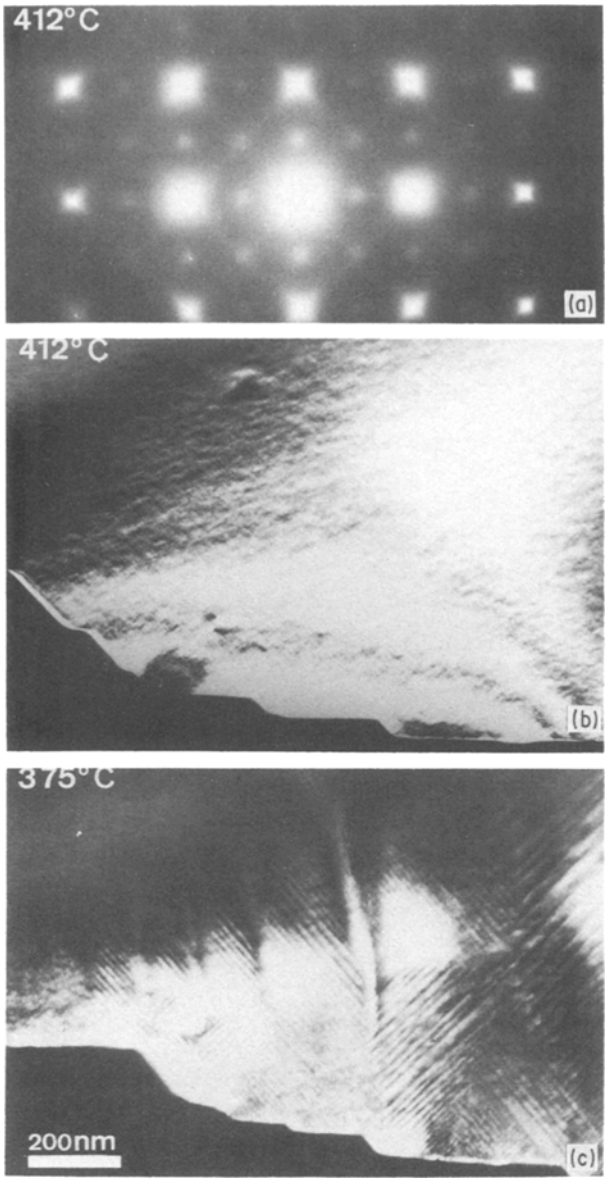

Figure 10 In situ heating sequence in CuAu. (a) [0 0 1] diffraction pattern above T_c. (b) 2 0 0 dark-field above T_c; note the presence of an intense tweed. (c) The same area as in (b) after cooling to 375° C. The ordering proceeds very fast.

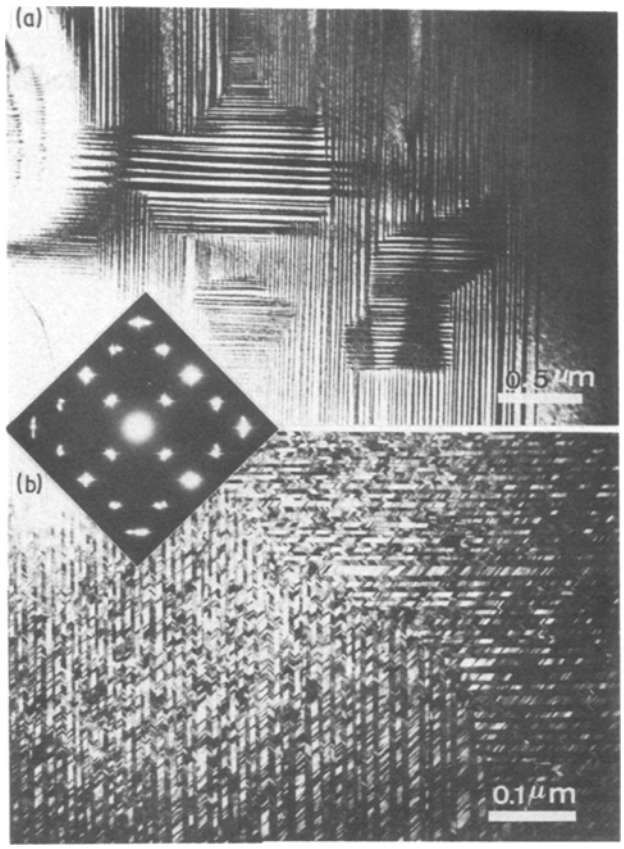

Figure 11 In situ heating sequence in CuAu. The quenched material has been heated above T_c and slowly cooled to room temperature inside the microscope: (a) low magnification; (b) higher magnification. Note that only two variants are present in the image as well as on the electron diffraction pattern.

microdomains; however, it should be noted that the resolution of the microscope at this temperature was certainly not better than 1 nm. Upon cooling an intense "shimmering" is observed and quite suddenly around 375° C the tweed seems to freeze in and narrow ordered domains form, elongated along (1 0 1) (see Fig. 10c). The ordered domains grow fast forming an attractive mosaic pattern (Fig. 11) where again only two

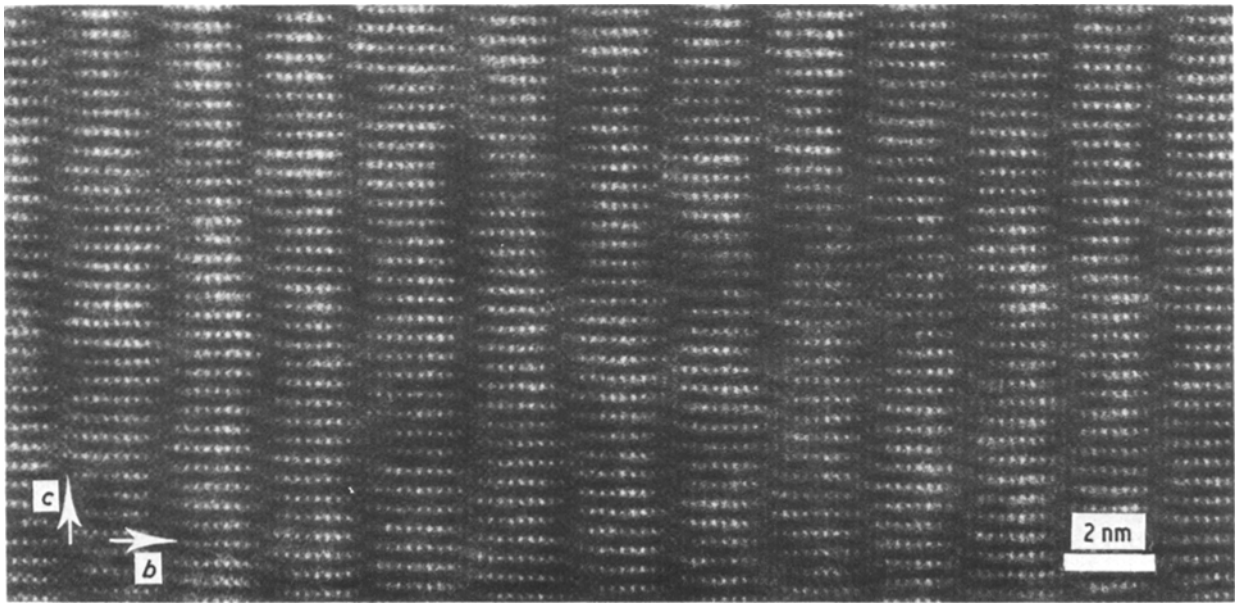

Figure 12 High-resolution image of wavy antiphase boundaries in CuAuII imaged along the [1 0 0] direction (cf. Fig. 1c).

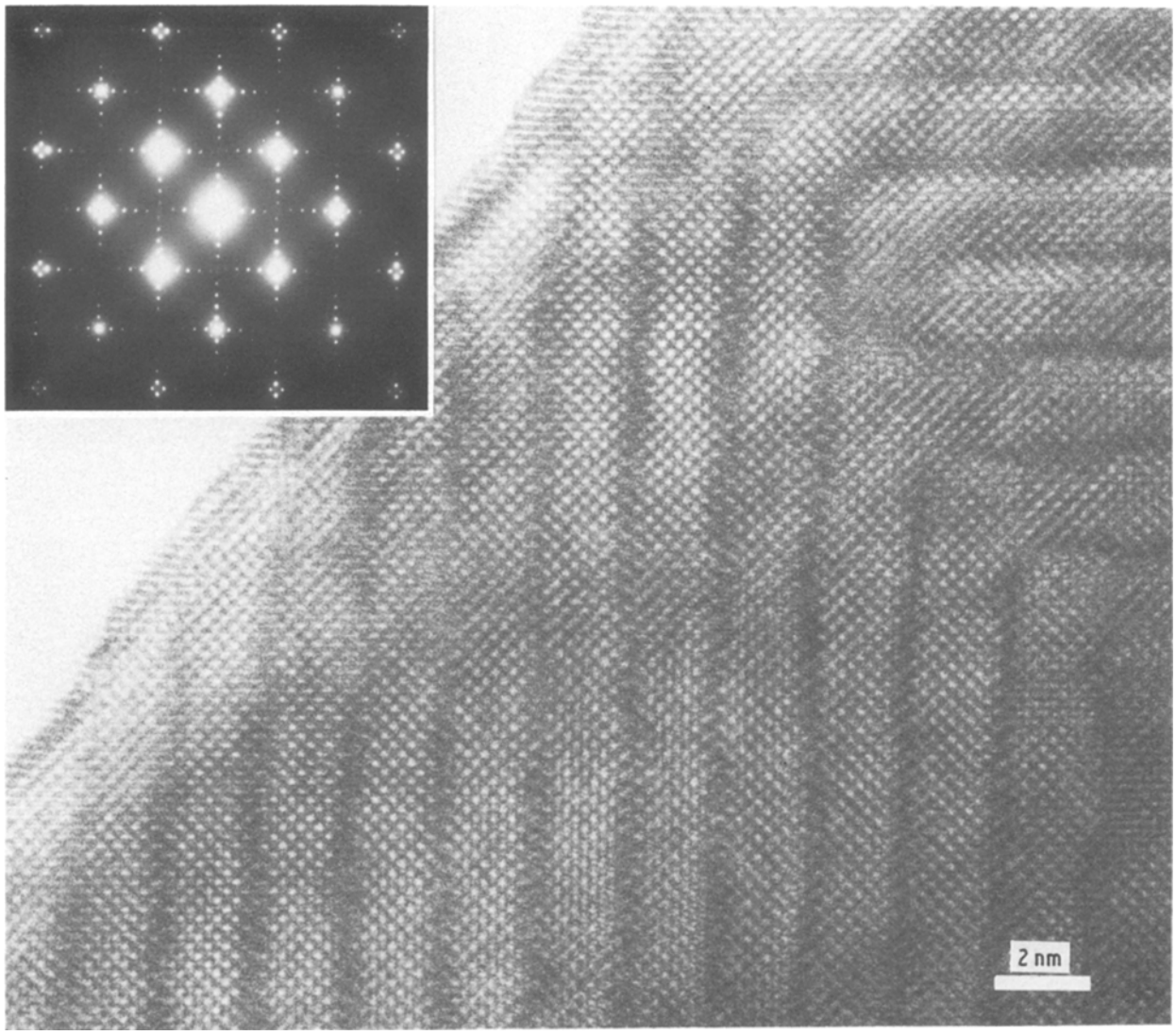

Figure 13 High-resolution image of periodic APBs in a CuAuII plate (cf. the schematic representation in Fig. 1d). The diffraction pattern which shows a slight orientation and spacing anomaly ($M \approx 5.12$) is also represented.

orientation variants are formed. Twin boundaries are along (1 0 1) planes and antiphase boundaries inside the twin lamellae are along (1 0 0) type planes. The c/a ratio deduced from electron diffraction patterns of CuAu formed in these thin foils is the same as that observed in bulk specimens. The transformation is completely reversible and the specimen can be cycled several times, the details of the pattern of domains change of course.

6. The fine structure of antiphase boundaries in CuAuII

High-resolution images have been obtained from the periodic antiphase boundary structure in CuAuII precipitates. The structure has been imaged along the three cube directions. In the [0 1 0] section where the long period is parallel to the electron beam no ordering effect is observed since along the [0 1 0] beam direction gold columns interchange with copper columns every time an APB is crossed. More useful information is obtained along [1 0 0] and [0 0 1] (see Figs 12 and 13, respectively). Both images show configurations of bright dots which correspond in orientation and separation with the copper (or gold) configuration in the CuAuII structure. The APBs which are separated by approximately 2.0 nm are recognized as dark lines. It is important to note that these APBs are imaged as diffuse lines, along which the bright dot configurations present on both sides of the interface fade out. This effect becomes more pronounced for increasing thickness.

Structure image calculations have been carried out with the help of the real space method [19, 20] to support the atomistic interpretation of the bright dot configuration. If a perfect long period structure (such as the one in Fig. 1, with all atom positions on a copper sublattice occupied by copper atoms and all positions on a gold sublattice occupied by gold atoms) is computer simulated, a sharp interface will result without any diffuse atom planes. Such calculations have explicitly been carried out for Cu–Pd alloys where similar diffuse APBs were observed [21]. Experimentally, sharp, well-defined and straight periodic APBs have been observed in, for example, Au–Mn [22], Ag_3Mg [23] or Cu–Al [24]. Accurate X-ray measurements by Okamura *et al.* [5] have indicated that not only a slight lattice relaxation is associated with the periodic interfaces but mainly that disorder

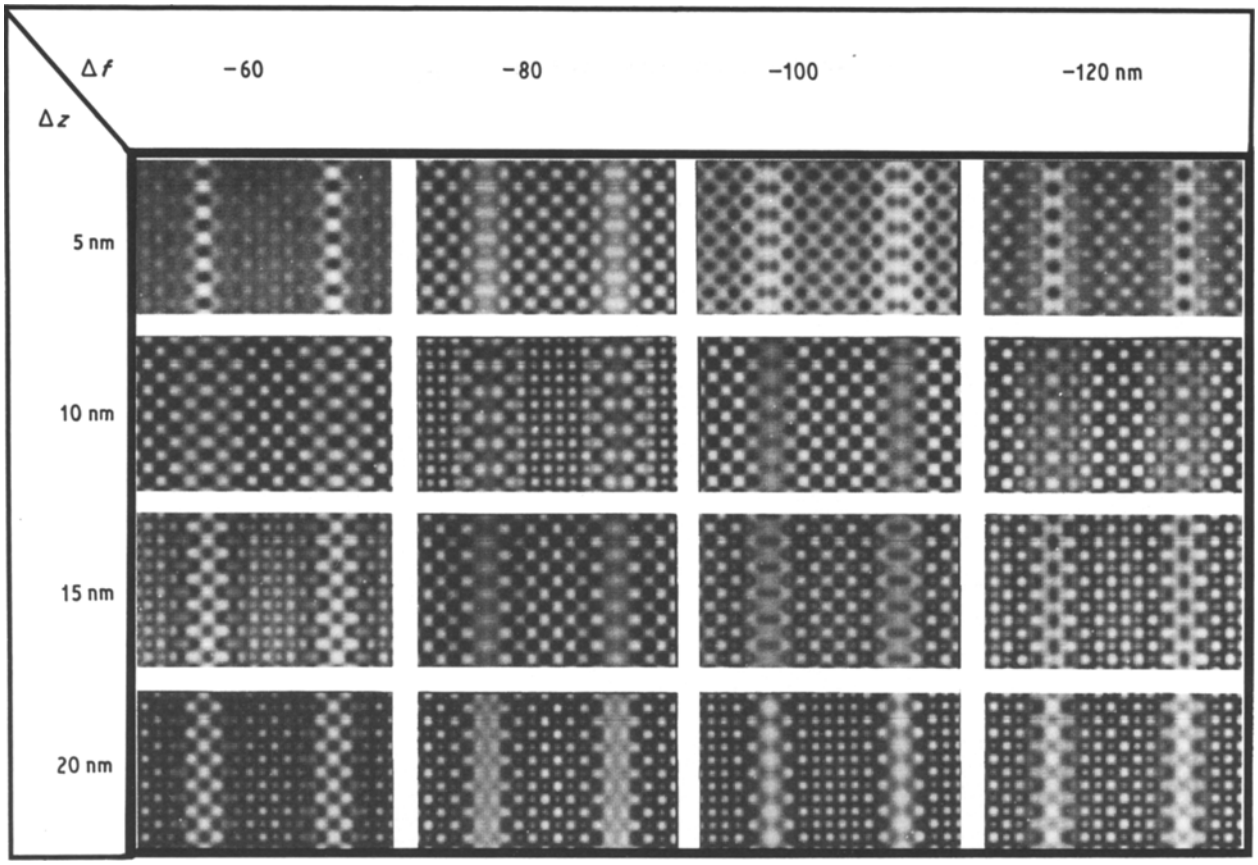

Figure 14 Calculated HREM images of CuAuII according to the model of Okamura *et al.* [5] for different thicknesses and defocus values.

has to be assumed along the antiphase boundaries. This seems to be inherent to the CuAuII structure, even for a stoichiometric composition. The copper positions next to the interface are only for 70% occupied by copper atoms (and for 30% by gold atoms); the next nearest copper positions contain already 94% Cu; the disorder is therefore mainly restricted to one atomic plane on each side of the interface. When this disorder is taken into account for the structure image calculations along [0 0 1], a diffuse APB line will indeed result (see Fig. 14 for different focus and thickness values). Dependent upon the focus, copper or gold positions may be imaged as bright dots. Therefore when the experimental parameters of focus and thickness are not accurately known it cannot be concluded which species is imaged as a bright dot. A good agreement between observed and calculated images is obtained for defocus values between −80 and −100 nm.

From the present observations it can therefore be concluded that the diffuse character of the APB images is due to a decrease of order along the boundaries. It cannot be explained by lattice relaxation only. This assumption has been thoroughly tested for Cu–Pd where several trial structures with and without relaxation and/or disorder have been used as an input for the structure image programme [21].

Apart from the disorder along the interface, the APBs are also not straight. Only on average are they lying in {1 0 0} planes; locally they may deviate by one or two interatomic distances from a given cube plane. These "wavy" boundaries are clearly observed in Fig. 13; they have already been observed by Guymont *et al.* [25] following a suggestion by Jehanno and Pério [2]. The wavy character of the APBs is also responsible for the fact that at larger thicknesses the diffuse character seems to increase; the boundaries in Fig. 13 are also wavy along the imaging direction [0 0 1] and therefore copper columns will continue as gold columns when intersected by an APB.

In the electron diffraction pattern of Fig. 13, up to six satellites on both sides of the basic reflections can be observed. The measured M value is $M = 5.12 \pm 0.02$), i.e. clearly incommensurate with respect to the basic lattice. However, with the present idea of the wavy and disordered APB structure this can hardly be a surprise.

Acknowledgement

G. Van Tendeloo is grateful to Dr L. Tanner for the many stimulating discussions.

References

1. M. GUYMONT and D. GRATIAS, *J. Phys. Lett.* **39** (1978) 437.
2. G. JEHANNO and P. PÉRIO, *J. Phys. Radium* **23** (1962) 854.
3. M. GUYMONT, D. GRATIAS and A. BISSON, *Phys. Status Solidi (a)* **54** (1979) 573.
4. C. H. JOHANNSON and J. O. LINDE, *Ann. Physik* **25** (1936) 1.
5. K. OKAMURA, H. IWASAKI and S. OGAWA, *J. Phys. Soc. Jpn.* **24** (1968) 569.
6. M. TAKEDA and H. HASHIMOTO, *Phys. Status Solidi (a)* **87** (1985) 141.
7. M. HIRABAYASHI and S. WEISSMANN, *Acta Metall.* **10** (1962) 25.
8. H. I. AARONSON and K. R. KINSMAN, *ibid.* **25** (1977) 367.

9. J. S. BOWLES and C. M. WAYMAN, *ibid.* **27** (1979) 833.
10. R. SMITH and J. S. BOWLES, *ibid.* **8** (1960) 405.
11. J. DUTKIEWICZ and G. THOMAS, *Met. Trans.* **6A** (1975) 1919.
12. G. VAN TENDELOO, S. AMELINCKX and D. DE FONTAINE, *Acta Crystallogr.* **B41** (1985) 281.
13. L. E. TANNER, *Phil. Mag.* **14** (1966) 111.
14. I. M. ROBERTSON and C. M. WAYMAN, *ibid.* **48** (1983) 421.
15. *Idem, ibid.* **48** (1983) 443.
16. *Idem, ibid.* **48** (1983) 629.
17. I. M. ROBERTSON and C. M. WAYMAN, *Met. Trans.* **A15** (1984) 269.
18. J. M. PENISSON, A. BOURRET and PH. EURIN, *Acta Metall.* **19** (1971) 1195.
19. D. VAN DYCK, *J. Microscopy* **119** (1980) 141.
20. *Idem, ibid.* **132** (1983) 31.
21. D. BRODDIN, G. VAN TENDELOO, J. VAN LANDUYT, S. AMELINCKX, R. PORTIER, M. GUYMONT and A. LOISEAU, *Phil. Mag.* in press.
22. G. VAN TENDELOO and S. AMELINCKX, *Phys. Status Solidi (a)* **65** (1981) 431.
23. R. PORTIER, D. GRATIAS, M. GUYMONT and W. M. STOBBS, *Acta Crystallogr.* **A36** (1980) 190.
24. N. KUWANO, H. MISHIO, M. TOKI and T. EGUCHI, *Phys. Status Solidi (a)* **65** (1981) 341.
25. M. GUYMONT, R. PORTIER and D. GRATIAS, *Acta Crystallogr.* **A36** (1980) 792.

Received 3 February
and accepted 14 March 1986